ISBN: 978-3-95450-234-9 ISSN: 2673-5504 doi:10.18429/JACoW-SRF2023-MOPMB033

EFFORTS TO SUPPRESS FIELD EMISSION IN SRF CAVITIES AT KEK

Mathieu Omet†, Hayato Araki, Takeshi Dohmae, Hayato Ito, Ryo Katayama,
Kensei Umemori, Yasuchika Yamamoto
High Energy Accelerator Research Organization, Tsukuba, Japan

Abstract

Our main objective is to achieve as high as possible quality factors Q0 and maximal accelerating voltages Eacc within superconducting radio frequency (SRF) cavities. Beside an adequate surface treatment, key to achieve good performance is a proper assembly in the clean room prior cavity testing or operation. In this contribution we present the methods and results of our efforts to get a better understanding of our clean room environment and the particulate generation caused during the assembly work. Furthermore, we present the measures taken to suppress filed emission, followed by an analysis of vertical test results of the last six years.

INTRODUCTION

Superconducting radio frequency (SRF) cavities [1] are state-of-the-art technological components utilized in accelerators worldwide. The primary parameters that determine their performance are the unloaded quality factor Q0 and the acceleration gradient Eacc. Field emission (FE) [2] can have detrimental effects on both parameters. Particulate contaminations can act as potent field emitters. Therefore, it is imperative to prevent the deposition of particulates on the inner surface of the cavity. Particulate contaminations can originate from two sources: the environment, such as particulates present in the clean room, and the generation during the assembly process. Understanding the cleanliness of the environment is crucial to identify areas for improvement. Similarly, comprehending the mechanisms of particulate generation and their movement during the assembly process is essential. In this proceeding, we discuss the efforts undertaken to address these issues. We also provide information on additional measures employed to suppress FE, as well as statistics on FE over the last six years.

CAVITY PREPARATION AND TEST CYCLE

Upon the production or receipt of a new cavity, the initial action involves conducting an optical examination of the inner surface using the Kyoto camera [3]. Subsequently, bulk electro polishing (EP), known as EP1, is applied, where a 100 µm layer is removed from the cavity's surface [4]. Afterwards, a high-pressure rinsing (HPR) with ultrapure water is carried out. This is succeeded by annealing, e.g. at a temperature of 900 °C for a duration of 3 hours.

The typical cycle for cavity preparation and testing proceeds as follows: The cavity undergoes optical inspection using the Kyoto camera. If any defects are detected, localized grinding is performed. The cavity is then transferred to the tuning machine, where frequency, field flatness, and straightness are measured and, if necessary, adjusted. In the subsequent step, EP2 and HPR processes are employed. After the HPR, the cavity is directly transferred to the clean room for assembly. Subsequently, the cavity is connected to a pumping station and leak checked. If the cavity passes this test, it is baked, e.g. at a temperature of 120 °C for 48 hours [5]. Finally, the cavity is moved to the vertical test (VT) stand, where it is tested at temperatures of 4 K and 2 K.

CLEAN ROOM SURVEY

To assess the level of cleanliness within a clean room, commonly a particle counter is set up at various positions and heights. Particle counts are then recorded over specific time intervals. However, in the studies detailed below, a novel approach was adopted by utilizing two different light sources (spot light and ViEST D Light Type F, provided by Shin Nippon Air Technologies (SNK) [6]), enabling the inspection of surfaces. In preparation for the subsequent studies, the ambient lights within the clean room were turned off. Due to the presence of large windows in most of the clean room walls, a certain amount of ambient light persisted.

In the direct comparison of the spot light and the D Light the latter one proved to be more versitle. With its light specturm primarily centered around violet, extending into the ultraviolet range, it enables the observation of contaminants and stains containing fluorescent components.

Using the D Light we investigated a total of 564 different surfaces within the following areas were investigated: changing room at the Center of Innovation (COI), COI class 1000 clean room, COI class 10 clean room, the changing room at the Superconducting RF Test Facility (STF), STF class 1000 clean room, and STF class 10 clean room.

In the changing rooms at both facilities, a substantial amount of dust and stains were discovered. Additionally, the walls of the air locks equipped with air showers exhibited dust accumulation. Furthermore, dust particles were visible on the majority of surfaces in both clean rooms, with notable areas of concern being tools and tool trays. Beside this, dust particulates were present on surfaces where items were stored on shelves, as well as on devices such as pumping stations and ultrasonic baths.

Based on the findings of this study, it was concluded that cleaning of certain surfaces was necessary. Following the cleaning procedures involving alcohol wiping and dry blowing, windows within the STF class 1000 clean room exhibited no visible dust particles.

† mathieu.omet@kek.jp

ISBN: 978-3-95450-234-9 ISSN: 2673-5504 doi:10.18429/JACoW-SRF2023-MOPMB033

Given the impracticality of cleaning the entire clean rooms with all the items present, it is crucial to prevent the whirling up of dust from areas behind shelves or tools such as torque wrenches. Additionally, items stored within the clean rooms must be cleaned prior to their use.

STUDY ON PARTICLE GENERATION DURING ASSEMBLY

The objective of this study was to gain insights into the generation, distribution, and dynamics of particles during the assembly process of a 9-cell TESLA-type cavity. Together with SNK employees, we positioned a green laser emitter in the STF class 10 clean room [7]. The laser beam was fanned out and directed through a specific area of interest. Particles that fell or floated through the laser beam caused light scattering, which was captured by a narrow-band video camera. To enable laser operation, all windows in the surrounding class 1000 clean room were shaded. This measure also improved the signal-to-background/noise ratio.

The tests described below represent a selection from a larger set of conducted experiments.

In one configuration, the expanded laser beam passed just in front of and below the input coupler port. The port was sealed using a blank flange and an O-ring. During the recording process, the flange, port, and the surrounding area were cleaned by using an ion gun for dry blowing. Simultaneously, a handheld particle counter was employed, which detected fewer than 10 particles in total. However, the video footage revealed scattered light from numerous particles, as shown in Fig. 1. Most particles exhibited fast movement with a downward trajectory.

Figure 1: Scattered light of particulates passing through fanned out laser beam during clean blowing. Composite picture of a 15 second video.

In the subsequent stage, the bolts securing the blind flange were loosened, and during this process, the scattered light emitted by numerous slowly moving particles was captured (see Fig. 2). Most of these particles exhibited floating motion, with both upward and downward movements.

Figure 2: Release of bolts of blind flange using a hex key and hands. Composite picture of a 15 second video.

Upon removing the blind flange, an L-shaped vacuum pipe, connected to a vacuum valve, was assembled to the coupler input port. As the bolts were tightened, the video recording showed the generation and release of many particles (see Fig. 3). These particles were observed floating in the air, predominantly with a downward trajectory, but some upward floating particles were also detected.

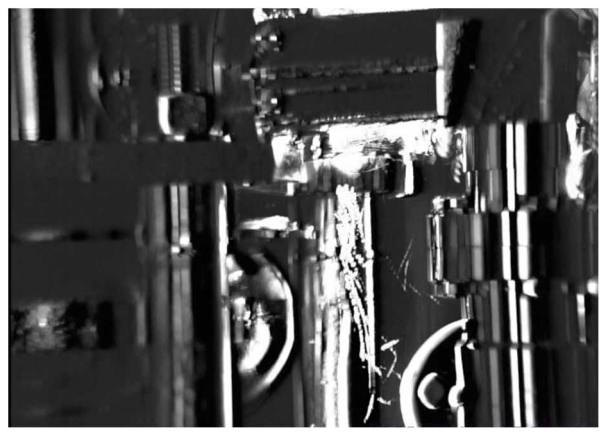

Figure 3: Tightening a bolt of the attachment using a hex key. Composite picture of a 20 second video.

Based on this study, we could deduce that the hand-held particle counter only provides a rough estimate of the actual particle concentration within the working area. Its small inlet nozzle is not capable of drawing in a sufficient volume of air to accurately measure particles. Additionally, we confirmed the critical importance of thorough cleaning in the working area. Furthermore, adopting slow and careful movements can help prevent the release of particles from the clean wear surface.

FURTHER MEASURES TO REDUCE FIELD EMISSION

In addition to optimizing the assembly process, we have implemented additional measures to minimize field emission.

ISBN: 978-3-95450-234-9 ISSN: 2673-5504 doi:10.18429/JACoW-SRF2023-MOPMB033

Typically, the irises of the cavity undergoing assembly and testing are subjected to grinding. The objective is to eliminate any surface defects present and to smoothen the surface. Subsequently, an EP2 process is performed, which has proven to rarely introduce new surface defects.

To further reduce field emission, we replaced the ion gun previously utilized in the STF class 10 clean room. The Simco Top Gun has been substituted with the Keyence SJ-L005G.

Furthermore, the scroll pumps at both the pumping station in the STF class 1000 clean room and the STF vertical test stand have been replaced with dry pumps.

FIELD EMISSION STATISTICS

Improving the assembly method, required tools and devices is a continuous and lengthy process. In order to assess the overall effectiveness of our endeavors, we conducted an evaluation of cavity vertical test data spanning from January 2017 to June 2023. The evaluation focused on key parameters, namely the gradient at which field emission occurred (onset) and the maximum achievable acceleration gradient. Only data from the final π-mode measurement at 2 K was considered. The evaluation was conducted separately for three distinct types of cavities: single cell, 3-cell, and 9-cell cavities. As each type presents its own unique challenges due to varying geometries, separate assessments were performed for accurate analysis and comparison.

Single-cell Cavities

The number of single-cell vertical cavity tests evaluated is 127 (see Fig. 4). 91 tests (71.7%) did not show any field emission. For the remaining 36 tests (28.4%) the average onset gradient is 27.2 MV/m. One can see a clear reduction of FE occurring over time, leading to zero FE cases in 2023.

When plotting the maximal Eacc and onset Eacc versus the assembly count, one can see that with the increasing assembly count the occurrence of FE is drastically reduced. The spread of the maximal Eacc narrows in a high gradient regime (see Fig. 5). The figure shows many data points at an assembly number of 0. This is due to the fact that the history of earlier cavity assemblies has not been reconstructed and transferred to a digital database yet.

When looking at the histogram of the maximal gradients, one can see a maximum around 36 MV/m (see Fig. 6 a)). It should be kept in mind that the depicted data is the result of R&D on many different cavities with a variety of different surface treatments. In case of single-cell cavities FE occurred mostly at moderate and very high gradients (see Fig. 6 b)).

Figure 7 shows how many of the treated and tested single-cell cavities reached which gradient regardless of FE and without FE. 90% of the tested cavities would fulfil LCLS-II specifications of 16 MV/m and 39% ILC specifications of 31.5 MV/m, in both cases without FE.

3-cell Cavities

The number of 3-cell vertical cavity tests evaluated is 14 (see Fig. 8). 7 tests (50.0%) did not show any field emission. For the remaining 7 tests (50.0%) the average onset gradient is 22.7 MV/m. Both, the onset gradient and the maximal acceleration gradient show a clear positive trend.

In case of the 3-cell cavities also the maximal Eacc and onset Eacc versus assembly count shows a clear positive trend (see Figure 9).

The histogram of the maximal Eacc has its maximum at 42 MV/m (see Fig. 10 a)). The cases of FE are dominant for the lower end of maximal Eacc (see Fig. 10 b)).

Figure 11 shows how many of the treated and tested 3-cell cavities reached which gradient regardless of FE and without FE. 93% of the tested cavities would fulfil LCLS-II specifications of 16 MV/m and 57% ILC specifications of 31.5 MV/m, in both cases without FE.

9-cell Cavities

The number of 9-cell vertical cavity tests evaluated is 67 (see Fig. 12). 16 tests (23.9%) did not show any field emission. For the remaining 51 tests (76.2%) the average onset gradient is 18.2 MV/m. Although the spread is quite large, for both, for the onset gradient and the maximal acceleration gradient, a positive trend can be seen from May 2019 until January 2022. From February 2022 on the trend was not followed. Most of it can be explained with new R&D on cavities and tests of cavities with known issues.

The maximal Eacc and onset Eacc versus assembly count both show a clear positive trend (see Fig. 13). The maximal Eacc distribution narrows down around the high gradient regime. Also in this case, it should be noted, that the data points shown at an assembly number of 0 are early cavity tests of which the history has not been reconstructed and transferred to a digital database yet.

The histogram of the maximal Eacc shows its maximum around 30 MV/m (see Fig. 14 a)). FE occurs for the entire range of maximal Eacc (see Fig. 14 b)).

Figure 15 shows how many of the treated and tested 9-cell cavities reached which gradient regardless of FE and without FE. 66% of the tested cavities would fulfil LCLS-II specifications of 16 MV/m and 9% ILC specifications of 31.5 MV/m, in both cases without FE.

Comparison

With the number of cells per cavity, the number of vertical tests showing field emission is increasing (see Fig. 16 a)). At the same time the average onset gradient decreases with the number of cells per cavity (see Fig. 16 b)). The reason for this is most likely the increased inner surface area as well as the complexity of the cavity shape. E.g., single-cell cavities have less ports (only 2) compared to 9-cell cavities (6 ports plus complicated structures such as the higher order mode (HOM) couplers).

ISBN: 978-3-95450-234-9 ISSN: 2673-5504 doi:10.18429/JACoW-SRF2023-MOPMB033

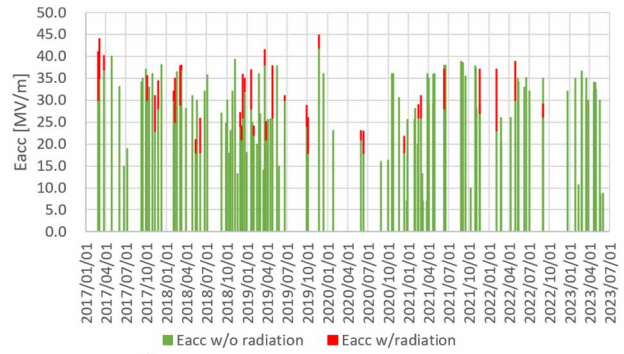

Figure 4: Maximum accelerating gradient over time for VTs of single-cell cavities. The red part of the bars indicates FE.

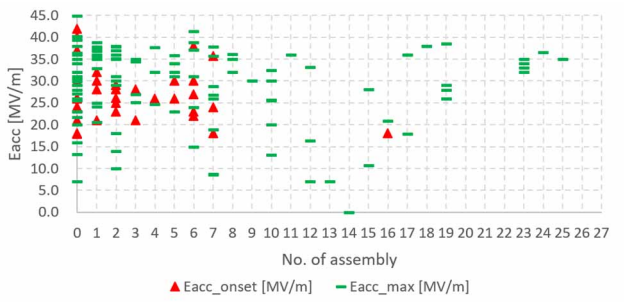

Figure 5: Maximal Eacc (green bars) and onset Eacc (red triangles) versus assembly count for single-cell cavities.

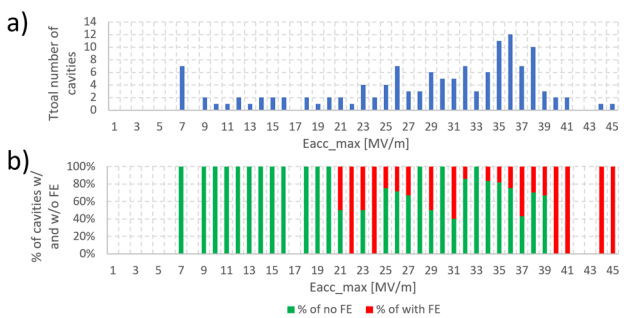

Figure 6: a) Histogram of maximal Eacc for single-cell cavities, b) percent of FE occurrence per maximal Eacc reached.

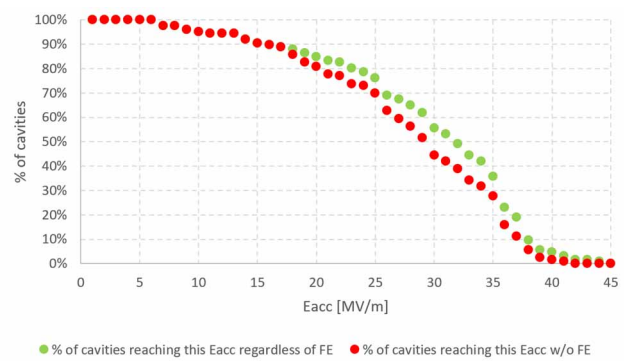

Figure 7: Percentage of single-cell cavities reached the corresponding Eacc regardless FE (green) and without FE (red).

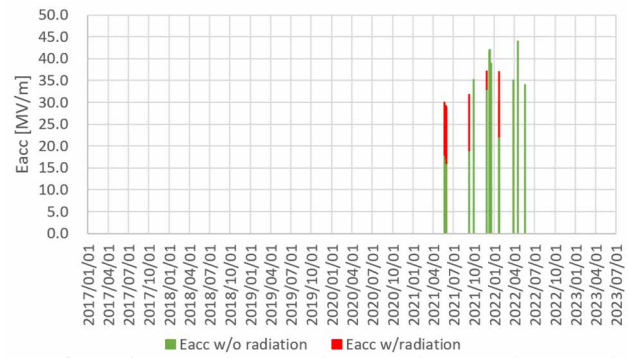

Figure 8: Maximum accelerating gradient over time for VTs of 3-cell cavities. The red part of the bars indicates FE.

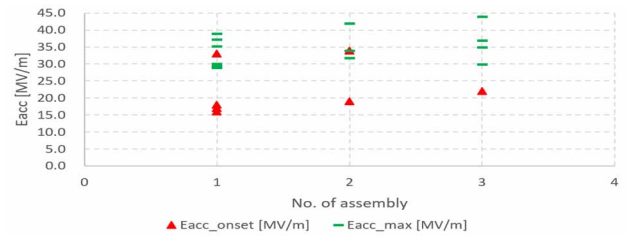

Figure 9: Maximal Eacc (green bars) and onset Eacc (red triangles) versus assembly count for 3-cell cavities.

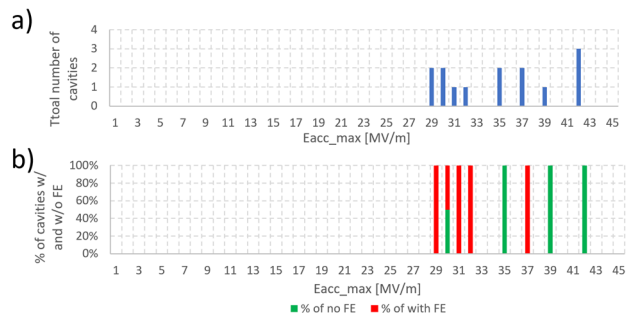

Figure 10: a) Histogram of maximal Eacc for 3-cell cavities, b) percent of FE occurrence per maximal Eacc reached.

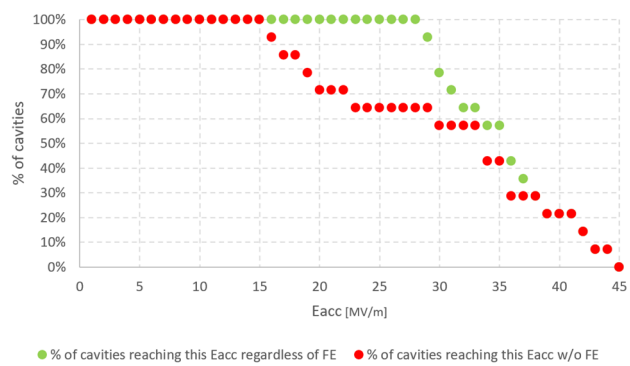

Figure 11: Percentage of 3-cell cavities reached the corresponding Eacc regardless FE (green) and without FE (red).

ISBN: 978-3-95450-234-9 ISSN: 2673-5504 doi:10.18429/JACoW-SRF2023-MOPMB033

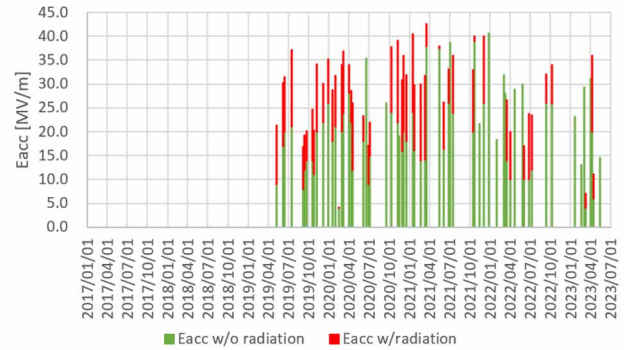

Figure 12: Maximum accelerating gradient (green bars) and onset gradient (red triangles) over time for VTs of 9-cell cavities.

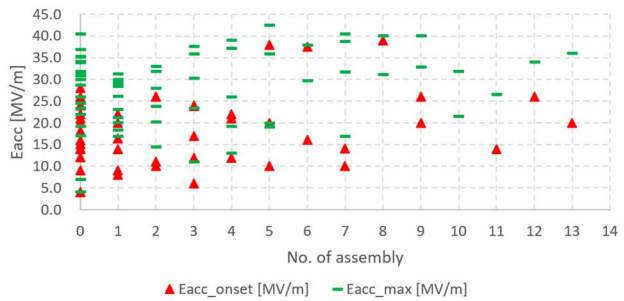

Figure 13: Maximal Eacc (green bars) and onset Eacc (red triangles) versus assembly count for 9-cell cavities.

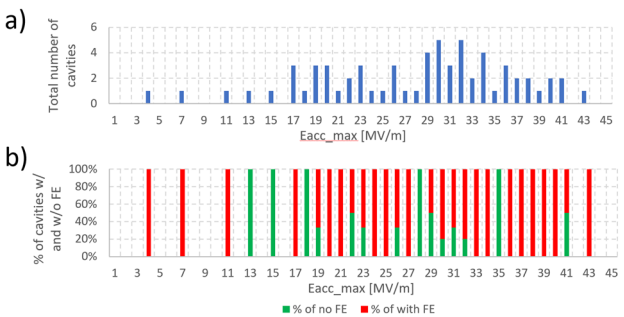

Figure 14: a) Histogram of maximal Eacc for 9-cell cavities, b) percent of FE occurrence per maximal Eacc reached.

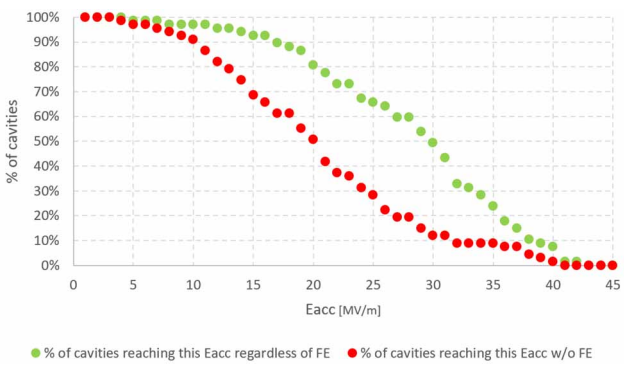

Figure 15: Percentage of 9-cell cavities reached the corresponding Eacc regardless FE (green) and without FE (red).

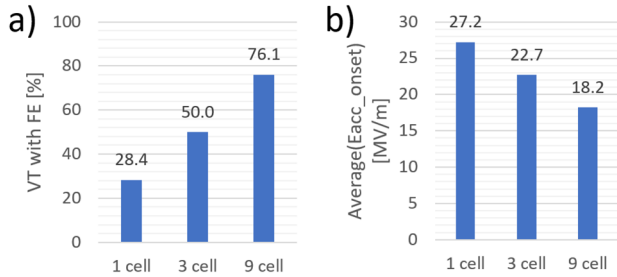

Figure 16: Comparison of single cell, 3-cell, and 9-cell cavity tests: a) percent of tests showing FE, b) average onset gradient.

CONCLUSION

Suppressing field emission in SRF cavities is a multifaceted endeavour. Two crucial aspects involve the removal of surface defects and the prevention of inner surface contamination. To address the first aspect, we employ a suitable approach that includes iris grinding followed by EP. The second aspect is influenced by various factors, such as the cleanliness of the environment, particulate generation during tool usage, particulate production within devices, and the overall quality of the assembly process. We consistently evaluate and improve our procedures and tooling to prevent or at least minimize potential surface contamination.

REFERENCES

[1] H. Padaesee *et al.*, *RF Superconductivity for Accelerators,* 2nd Edition, ISBN: 978-3-527-40842-9, Hoboken, NJ, U.S., Wiley, 2008.

[2] H. Padaesee *et al.*, "*RF* Field Emission in Superconducting Cavities", in *Proc. SRF'87,* Lemont, IL, USA, Sep. 1987, paper SRF87C03, pp. 251-272.

[3] Y. Iwashita *et al.*, "Development of High Resolution Camera for Observations of Superconducting Cavities", *Phys. Rev. ST Accel. Beams*, vol. 11, p. 093501, Sep. 2008. doi:10.1103/PhysRevSTAB.11.093501

[4] E. Kako *et al.*, "Improvement of Cavity Performance by Electro-Polishing in the 1.3 GHz Nb Superconducting Cavities", *in Proc. PAC'99,* New York, NY, USA, Mar. 1999, paper THAL6, pp.432-434.

[5] G. Ciovati et al., "High field Q slope and the baking effect: Review of recent experimental results and new data on Nb heat treatments", *Phys. Rev. ST Accel. Beams*, vol. 13, p. 022002, Feb. 2010. doi: 10.1103/PhysRevSTAB.13.022002

[6] SNK, https://www.snk.co.jp/particle/prouct5.html

[7] SNK, https://www.snk.co.jp/particle/engineering1.html